

# Study of gas–liquid mixing in stirred vessel using electrical resistance tomography

Sher, F., Sajid, Z., Tokay, B., Khzouz, M. & Sadiq, H.

**Author post-print (accepted) deposited by Coventry University's Repository**

**Original citation & hyperlink:**

Sher, F, Sajid, Z, Tokay, B, Khzouz, M & Sadiq, H 2016, 'Study of gas–liquid mixing in stirred vessel using electrical resistance tomography' *Asia-Pacific Journal of Chemical Engineering*, vol. 11, no. 6, pp. 855-865.  
<https://dx.doi.org/10.1002/apj.2019>

DOI 10.1002/apj.2019

ISSN 1932-2135

ESSN 1932-2143

Publisher: Wiley

**This is the peer reviewed version of the following article: Sher, F, Sajid, Z, Tokay, B, Khzouz, M & Sadiq, H 2016, 'Study of gas–liquid mixing in stirred vessel using electrical resistance tomography' *Asia-Pacific Journal of Chemical Engineering*, vol. 11, no. 6, pp. 855-865. which has been published in final form at <https://dx.doi.org/10.1002/apj.2019>. This article may be used for non-commercial purposes in accordance with Wiley Terms and Conditions for Self-Archiving.**

**Copyright © and Moral Rights are retained by the author(s) and/ or other copyright owners. A copy can be downloaded for personal non-commercial research or study, without prior permission or charge. This item cannot be reproduced or quoted extensively from without first obtaining permission in writing from the copyright holder(s). The content must not be changed in any way or sold commercially in any format or medium without the formal permission of the copyright holders.**

**This document is the author's post-print version, incorporating any revisions agreed during the peer-review process. Some differences between the published version and this version may remain and you are advised to consult the published version if you wish to cite from it.**

# Study of gas-liquid mixing in stirred vessel using electrical resistance tomography

Farooq Sher<sup>a,e\*</sup>, Zaman Sajid<sup>b,e</sup>, Begum Tokay<sup>a</sup>, Martin Khzouz<sup>c,e</sup>, Hamad Sadiq<sup>d,e</sup>

*a. School of Chemical and Environmental Engineering, University of Nottingham, Nottingham NG7 2RD, UK.*

*b. Process Engineering, Faculty of Engineering and Applied Science, Memorial University of Newfoundland, NL, A1B 3X5 Canada.*

*c. School of Mechanical, Aerospace and Automotive Engineering, Faculty of Engineering, Coventry University, Coventry CV1 5FB, UK.*

*d. Institute of Chemical Engineering and Technology, University of the Punjab, Lahore, 54590, Pakistan.*

*e. Sustainable Energy, Environment and Climate Change Research Group (SEECG), Nottingham NG9 2JB, UK.*

## Abstract

This study presents a full operation and optimisation of a mixing unit; an innovative approach is developed to address the behaviour of gas-liquid mixing by using Electrical Resistance Tomography (ERT). The validity of the method is investigated by developing the tomographic images using different numbers of baffles in a mixing unit. This technique provided clear visual evidence of better mixing that took place inside the gas-liquid system and the effect of a different number of baffles on mixing characteristics. For optimum gas flow rate ( $\text{m}^3/\text{s}$ ) and power input (kW), the oxygen absorption rate in water was measured. Dynamic gassing-out method was applied for five different gas flow rates and four different power inputs to find out mass transfer coefficient ( $K_La$ ). The rest of the experiments with one up to four baffles were carried out at these optimum values of power input (2.0 kW) and gas flow rate ( $8.5 \times 10^{-4} \text{ m}^3/\text{s}$ ). The experimental results and tomography visualisations showed that the gas-liquid mixing with standard baffling provided near the optimal process performance and good mechanical stability, as higher mass transfer rates were obtained using a greater number of baffles. The addition of single baffle had a striking effect on mixing efficiency and additions of further baffles significantly decrease mixing time. The energy required for complete

---

\*Corresponding author. Tel.: +44 (0) 7472 550 250

E-mail addresses: [Farooq.Sher@nottingham.ac.uk](mailto:Farooq.Sher@nottingham.ac.uk), [Farooq.Sher@gmail.com](mailto:Farooq.Sher@gmail.com) (F.Sher)

27 mixing was remarkably reduced in the case of four baffles as compared to without any baffle. The  
28 process economics study showed that the increased cost of baffles installation accounts for less cost of  
29 energy input for agitation. The process economics have also revealed that the optimum numbers of  
30 baffles are four in the present mixing unit and the use of an optimum number of baffles reduced the  
31 energy input cost by 54%.

32 **Keywords:**

33 Gas–liquid mixing, hydrodynamics, mass transfer, tomography, stirred vessel, baffles, and process  
34 economics.

35 **1. Introduction**

36 From customarily unit operations, mixing is one of the most important process used in engineering  
37 and allied industries, which plays an important role in the commercial success of industrial operations.  
38 Fluid mixing has been extensively studied for many years. The major applications of mixing include  
39 in chemical and biotechnological industries, where single and multi-phase fluids are mixed in stirred  
40 tanks [1]. The process scale-up, design of a mixing equipment, energy input and mixing products  
41 quality depends on the flow behaviour of a stirred tank. Therefore, an understanding of such flow  
42 pattern is important [2].

43

44 Mechanically-stirred tanks are extensively used in the chemical and process industries, including  
45 applications in the production of chemicals, pharmaceuticals, foods, paper, minerals, metals and many  
46 others [3-6]. Typical operations which are usually carried out in mixing tanks include blending of  
47 liquids, contacting of a liquid with a gas or second immiscible liquid, solids suspension and chemical  
48 reactions. Despite many years of research and accumulated experience in the design of this important  
49 type of equipment, the fluid flow behaviour of stirred tanks still remains a subject of active  
50 investigation. The design of a stirred tank needs to be carefully matched to the particular operation,  
51 but due to the complex flow patterns encountered many uncertainties remain in the design and scale-  
52 up procedures. Operations involving multiphase mixtures, e.g. contacting of a liquid with a gas,

53 another immiscible liquid, particulate solids, or some combination of these, form a large proportion of  
54 stirred tank applications. For multiphase operations, there are significant additional complexities  
55 which need to be addressed, compared with single-phase liquid flow. Many of the uncertainties in  
56 design are related to multiphase aspects, and therefore, the focus of this study is on multiphase flow.  
57 More specifically, this study considers the case of gas–liquid contacting, which takes place on a pilot  
58 scale stirred vessel.

59

60 In the design and operation of stirring tanks, mass transfer is one of the vital phenomena, where  
61 agitation and aeration are influential variables to deliver an effective rate of mass transfer during the  
62 mixing process, it can be characterised and analysed by the means of mass transfer coefficient ( $K_{La}$ ).  
63 The values of  $K_{La}$  are affected by several features, including the geometry of the tank, type of  
64 impeller, agitation speed, aeration rate, media composition and properties [7]. The determination of  
65 the  $K_{La}$  in mixing is also crucial to baseline efficiency parameters and to quantify the optimum  
66 operating variables. The  $K_{La}$  for gas absorption is calculated using dynamic gassing–out method [8,  
67 9].

68

69 Many experimental studies have been undertaken over the years to investigate the characteristics of  
70 fluid flow in stirred tanks. Often, these studies have resulted in empirical correlations, which relate a  
71 global parameter, e.g. power draw, mixing time or mass transfer rate, the geometric configuration and  
72 operating conditions [10-14]. One approach for determining the details of internal flow is through  
73 experimental studies at laboratory scale. A range of advanced measurement methods [15-18] have  
74 been applied to get valuable information; whilst there are also various limitations. For example, it is  
75 very difficult to apply experimental methods to full-scale industrial tanks, and therefore, uncertainties  
76 during scale-up need to be addressed. Moreover, the experimental methods use model fluids (e.g.  
77 water and air), but real industrial processes potentially deal with fluids which show variations from  
78 ideal behaviours at high temperatures and pressures.

79

80 In recent research, the study of the flow behaviour of a system using its flow visualisation has gained  
81 momentum. Tomography is one of the many techniques, which provides the images of the contents  
82 within a closed system. The basic principle of electrical resistance tomography (ERT) is to take  
83 multiple measurements at the periphery of an equipment, vessel or pipeline and combine these to  
84 provide information on the electrical properties of the process volume. Since the mixing vessel is a  
85 closed system, ERT is implemented as a tool to investigate the mixing phenomena. ERT has also been  
86 utilised to study the mixing behaviour of gas-liquid-solid systems, fibre suspensions, pulp mixing,  
87 polymer particles mixing and many more [19-25]. But less has been written about the use of ERT to  
88 study the gas-liquid mixing phenomena [26].

89

90 In the present study, gas-liquid mixing in a mechanically stirred vessel was analysed by using ERT  
91 method. This technique applies currents or voltages and measures these parameters via electrodes  
92 fitted on the edges of the domain. The study is also novel in a sense that the effect of mixing on  
93 concentration is studied by changing the number of baffles. To determine the effectiveness of the  
94 results developed, the mixing curves were compared with the literature [27]. Moreover, a new  
95 instrumental platform for validation of optimum power and energy consumption in stirred vessel was  
96 also investigated. One of the most stimulating elements in the design is cost estimation to build and  
97 operate the system, for that process economics of the mixing unit was also studied to evaluate the  
98 power consumption, installation and operational cost.

## 99 **2. Experimental setup**

### 100 **2.1 Mixing unit**

101 The experimental arrangement is shown in Fig. 1. The mixing unit consisted of a transparent Plexiglas  
102 cylindrical vessel. The internal diameter ( $T$ ) was 0.217 m. The vessel was filled with water up to a  
103 height ( $H$ ) of 0.217 m. To prevent vortex and dead zones, the vessel was fitted with four equally  
104 spaced PVC baffles. The baffles used had the standard width of 0.022 m ( $T/10$ ) with a clearance of  
105 0.004 m ( $T/50$ ) to the vessel walls. ERT probe was constructed on one of these baffles. A standard

106 six blades Rushton turbine impeller with a diameter (D) of 0.072 m (T/3), width B= D/5 and height W  
107 = D/4 was used. The impeller off-bottom clearance C= T/3, was measured from impeller disc centre  
108 to the bottom of the vessel. A top entering impeller assembly was fitted in the vessel. A variable  
109 frequency drive (VFD) was used to change the impeller speed up to the desired rotational speed  
110 (rpm). A rotary torque transducer E202 torque meter was installed to measure impeller speed and  
111 torque. Gas flow was supplied via a sparger mounted centrally on the base of the vessel. The Gas  
112 sparger consisted of sixteen (16) air holes; each of them had a diameter of 1 mm, which gave a total  
113 area of  $1.256 \times 10^{-5} \text{ m}^2$  for holes. The circumference, which contained the holes, had a diameter of 0.06  
114 m. The ring sparger was positioned at a length of T/6 from the base of the mixing vessel. In addition  
115 to this, an electrical resistance tomography system and a computer was setup on the unit. The  
116 tomography system was made by Industrial Tomography System Manchester, United Kingdom (UK).

## 117 **2.2 Tomographic probe design and construction**

118 The tomographic probe was constructed on one of the baffles [28-31]. The tomographic probe was  
119 made of a 35-micron tin-clad copper foil. The foil was coated with an electrically conductive acrylic  
120 adhesive. This copper foil was selected due to its removable silicone liner, which was helpful for  
121 gluing on the plastic surface, the coating acrylic adhesive was a conductive, good high and low-  
122 temperature resistance, excellent resistance to ozone, oil, chemicals and water and at last, it was easily  
123 soldered. The electrodes dimensions were a function of the velocity of materials, diameter of the  
124 vessel, conductivity range under study. The required imaging speed was a function of the vessel's  
125 diameter, conductivity range to be measured, the velocity of the fluid and the required imaging speed.  
126 A vertical series of the electrodes of equal dimensions were arranged at the same distances on one of  
127 the baffles. The total length of one electrode used was 1.5 cm with a width 6 mm. In total 18  
128 electrodes of length 6 mm were used as a gap of 2 mm each. The electrodes were screwed and wired  
129 to the baffle, the design and actual constructed ERT probe is shown in Fig.2.

130

131 The two spare electrodes referred to as the ground or earth electrodes (one at the top and one at the  
132 bottom), which were located away from the measurement electrodes but were in electrical contact

133 with the fluid inside the vessel. It was made sure that all measurements of voltages were fixed against  
134 a common ground source. A co-axial cable was used to connect the data acquisition system (DAS)  
135 device with electrodes, which were in contact with the fluid inside the vessels. The outer coat of the  
136 co-axial cable is buckled to the feedback path of a buffer voltage to provide noise indemnity and the  
137 inner core was capacitively coupled to the input of the voltage buffer. This reduced the  
138 electromagnetic noise and interference. After the construction of this ERT linear probe, all the  
139 electrodes are separately checked by ohms meter. They were calibrated and tested with a standard  
140 solution and found, according to the standards and gave a good quality of results [28, 29, 31]. In the  
141 contiguous approach, two adjacent pair of electrodes was used to apply current. Voltage was  
142 measured through the remaining adjacent pair of electrodes, and an injection pair of electrodes was  
143 swapped to the next pair of electrodes and was repeated until all independent combinations were  
144 completed, according to Eq. 1, for a plan of sixteen electrodes it provides one hundred and four  
145 voltage individual measurements.

$$146 \quad M_e = \frac{n_e(n_e - 3)}{2} \quad (1)$$

147 Where  $M_e$  represents number of independent voltage measurements without those that were obtained  
148 with electrode(s), which were used for current injection and  $n_e$  represents the electrodes' number.  
149 Finally, the data was processed using ITS System 2000 Version 5.0 image rehabilitation algorithm in  
150 host image reconstruction unit, which communicates through DAS. The algorithms exist in the host  
151 computer connected to the DAS and used both on- and off-line depending on the time constraints and  
152 the type of image required. The distinction between the two algorithms is that one produces images  
153 depicting a change in resistivity relative to an initially acquired set of reference data, and the other  
154 produces an image depicting the values of resistivity or conductivity for each pixel [32].

### 155 **2.3 Experimental procedure**

156 The air and tap water were used, as gas phase and liquid phase fluids respectively throughout all the  
157 experiments. For every experiment, the vessel was filled up with water up to a height (H), equivalent  
158 to the vessel diameter (21.7 cm). Before each experiment, the oxygen of the water was removed by

159 means of a current of nitrogen. The flow rate of both gases was controlled by two separate installed  
160 valves. A Rotameter (METRIC 18XA) was used in the line to control and determine the rate of  
161 aeration. The concentration of dissolved oxygen in water was measured using an oxygen probe  
162 connected to bench microprocessor based logging meter (HANNA HI964400). The probe measured  
163 dissolved oxygen concentration with a sensor covered by a membrane and temperature with a built-in  
164 temperature sensor. When a voltage was applied across the sensor, the membrane allows oxygen to  
165 pass through and oxygen that had passed through the membrane caused a current flow. The air was  
166 supplied to the vessel from a combressor through a 6 mm diameter rubber piple. Before entering into  
167 the vessel, the air passed through a filter.

168

169 The data acquisition system P2000 is provided by ITS (Industrial Tomography System) was used. It  
170 had connectors to connect up to eight electrode planes, another connector for the power supply and  
171 one for the local earth was on the back. The individual plane of electrodes on the ERT sensor was  
172 connected to the device by the 36–way connectors.

173

174 Gas-liquid mass transfer measurements were performed without baffles at standard configurations; the  
175 system was fixed at four different power inputs as 1.0, 2.0, 3.0 and 5.0 kW; while air flow rates were  
176 changed as  $2.6 \times 10^{-5}$ ,  $1.0 \times 10^{-5}$ ,  $2.4 \times 10^{-4}$ ,  $5.0 \times 10^{-4}$  and  $8.5 \times 10^{-4}$  m<sup>3</sup>/s. The values of dissolved oxygen  
177 concentration were recorded at an interval of 10 s. Moreover, for each of the above pair, the mass  
178 transfer coefficients ( $K_{La}$ ) were calculated using dynamic gassing–out method [8, 9].

179

180 The power number  $N_p$  is used to describe the power consumption  $P$  of the stirrer. Power number  
181 depends on different factors which are mentioned in Eq. (2).

$$182 \quad N_p = \frac{P}{\rho N^3 D^5} \quad (2)$$

183 Where  $\rho$  is the density of the container fluid;  $D$  represents the impeller’s diameter and  $N$  refers to  
184 impeller rotational speed. Holland and Bragg (1995) revealed that with the help of Eq (3 ) and (4 ),  $N_p$   
185 can be correlated to degree of turbulence in tank, called Reynolds number  $N_{Re}$ , and Froude number  $Fr$ :

186

$$N_{\text{Re}} = \frac{\rho ND^2}{\mu} \quad (3)$$

$$F_r = \frac{N^2 D}{g} \quad (4)$$

189 Where  $\mu$  is the fluid viscosity,  $g$  is the gravitational acceleration. For a fully baffled single phase  
190 system, which is operating in the turbulent region, the effect of Froude and Reynolds numbers are  
191 dominated by inertial forces, which could be neglected. In the gassing process another important  
192 dimensionless number is the gas flow number  $F_g$ :

$$F_g = \frac{Q_g}{ND^3} \quad (5)$$

194 Where  $Q_g$  is sparger gassing rate. For the flow developing in the impeller zone, flow number is very  
195 important, which comprises the reaction of impeller diameter, rotating speed, and gassing rate but not  
196 dependent on the geometry of the blade.

## 197 **2.4 Process economics**

198 The cost of baffles and its installation cost was adopted from literature [33, 34]. The amount of energy  
199 input for no baffle, one, two, three and four baffles were also analysed. The amount of energy input  
200 for each case was converted into dollars spent to generate that energy. The cost data for energy input  
201 was adopted from literature [33]. Since the cost data was not updated in the reference list, the cost  
202 data was updated to the year 2014 using Chemical Engineering Plant Cost Index (CEPCI). The cost  
203 indexes for reference years were adopted from American Institute of Chemical Engineers (AIChE)  
204 website. A graphical relationship was developed to report the optimum number of baffles required for  
205 this system. The optimisation here is referred as the minimum cost, where the system provides or start  
206 to provide higher mass transfer efficiencies.

## 207 **3. Results and discussion**

### 208 **3.1 Hydrodynamics and gas–liquid mass transfer measurements**

209 In order to increase the reliability of the results, all experiments were run in triplicate and the results  
210 presented are averaged of all runs performed for each case. For optimum operation, hydrodynamic  
211 and mass transfer mechanisms are important to understand the mixing inside the vessel. Upon  
212 different power inputs, various flow patterns in the vessel were observed without any gas flow. Fig. 3,  
213 shows the Power number in terms of Reynolds number, it also represents some distinctive flow  
214 patterns inside the stirred vessel with standard Rushton turbine impeller.

215

216 The Power number was measured in the range of  $5 \times 10^3 < R_{Ne} < 7 \times 10^4$  over the Reynolds number also  
217 shown in Fig. 3, which displays a preliminary value of 90.8 which declines to 31.2 at a Reynolds  
218 number 15,120. Then it leftovers consistent decreasing with Reynolds number till it falls suddenly by  
219 43% to 9.8 at a Reynolds number value equal to 26,352; afterwards it varies a little with Reynolds  
220 number, with an average value of 4.75. This rapid fall in Power number with the Reynolds number is  
221 related with the rapid flow evolution from radial to axial, which was also witnessed visually during  
222 the experiment. This specific flow evolution was also noticed by Hockey *et al.* [35]. The plotted  
223 measurement are in good agreement with the others published literature [27].

224

225 The development of the  $K_{La}$  in terms of the gas flow rate, with various power configurations, was  
226 studied with the Rushton turbine impeller and is shown in Fig.4. The  $K_{La}$  value boosts with rising gas  
227 flow rates due to the augmented gas holdup. The effect is more significant for lower power inputs. For  
228 1.0 and 2.0 kW,  $K_{La}$  value continuously increasing when the gas flow rate is increased, and reached to  
229 0.075 and 0.085  $s^{-1}$ , respectively. However, when the power inputs are set to 3.0 kW and 4.0 kW, the  
230 rate of increase  $K_{La}$  is smaller, and there is no significant change in  $K_{La}$  value when the gas flow rate  
231 is set to  $5.0 \times 10^{-4} m^3/s$  and above.

232

233 For  $4.8 \times 10^{-4} \text{ m}^3/\text{s}$  gas feed, the highest  $K_{La}$  value of  $0.080 \text{ s}^{-1}$  was obtained for 4.0 kW. However, at  
234 the highest gas flow rate  $8.5 \times 10^{-4} \text{ m}^3/\text{s}$ , the maximum  $K_{La}$  value of  $0.085 \text{ s}^{-1}$  is recorded for 2.0 kW  
235 power input rather than for the highest power input 4.0 kW. Hence, the values of  $K_{La}$  are not so  
236 sensible to the variation of the power inputs in judgement with different air flow rates. An economic  
237 performance criterion was deduced from these  $K_{La}$  values in terms of the efficiency of the impeller at  
238 different power inputs. These optimum values of power input (2.0 kW) and gas flow rate ( $8.5 \times 10^{-4}$   
239  $\text{m}^3/\text{s}$ ) were used in the rest of the experiments by changing the number of baffles in ERT system.

### 240 **3.2 Effect of the number of baffles on gas–liquid mixing**

241 The degree of mixing with a changing number of baffles under gassed condition is represented in Fig.  
242 5. It clearly illustrates that insertion of baffles into the system can significantly improve the gas-liquid  
243 mixing with even standard Rushton turbine impeller. It was observed that without any baffle the  
244 maximum value of oxygen concentration 17.90 ppm was achieved though after 1020 s. The long  
245 duration of the oxygen concentration to reach a level of 17.90 ppm is due to none turbulence and less  
246 interfacial contact in the mixing region. Visual observations show that the tangential motion of the  
247 low viscosity liquid (water), imparted by rotating impeller has created a swirl, which has  
248 approximated solid body rotation producing inadequate mixing. Only one baffle has significantly  
249 reduced the blend time and also increases the oxygen concentration value. The oxygen concentration  
250 reached to 18.50 ppm as compared to 17.90 ppm of without baffling, which is a 3.35% increase in the  
251 maximum value of oxygen concentration.

252

253 Addition of the second baffle shows the dominant effect on oxygen concentration, which measured as  
254 19.20 ppm. That is, as compared to 17.90 ppm of without baffling, an increase of 7.26%. The addition  
255 of the first and the second baffles has greatly decreased the blending time, whilst addition of the third  
256 baffle has minimal effect on the oxygen concentration. Fig. 5 clearly shows that in the case of two  
257 baffles the maximum level of oxygen concentration was 19.20 ppm, which approaches to only 19.50  
258 ppm in the case of three baffles, 1.68% raise as compared to two baffles. The time to achieve the  
259 maximum level of oxygen concentration was 610 s when two baffles were employed, whereas it was

260 recorded as 590 s for three baffles. Furthermore, the addition of the fourth baffle achieved highest  
261 oxygen concentration (19.98 ppm), which corresponds to 11.6% increase in concentration from no  
262 baffle value (17.9 ppm). Also, the highest level of oxygen concentration was achieved in the shortest  
263 time 510 s. In the case of four baffles, system vortex formation was completely eliminated and the  
264 swirling motion was converted into the axial flow, which helps to achieve the maximum mass transfer  
265 and greater mechanical stability in gas–liquid mixing. Hence, by increasing the number of baffles  
266 break swirling and vortexing of liquid inside the vessel, and increase mixing and stabilizes the power  
267 drawn by reducing mixing time. Myers, Reeder *et al.* [36] predicted similar results output, while  
268 gas–liquid mixing in the study on optimise mixing by using the proper baffles.

### 269 **3.3 ERT for evaluating gas–liquid mixing**

270 In contemplation to get a more in-depth understanding about the gas-liquid mixing, ERT technique  
271 was used, which usually show the dispersal of the conductivity inside the mixing unit. The use of  
272 different colours combination helps to interpret the conductivity or eventually gas absorption in a  
273 specific area of the vessel [37]. In the present study, the gas phase oxygen (in air) was a conductive  
274 and liquid phase (tap water) was non-conductive without any dissolved oxygen. A typical set of  
275 tomograms was obtained using this technique which is shown in Fig. 6. These are based on the  
276 experiments conducted at an optimum power of 2.0 kW and gas flow rate of  $8.5 \times 10^{-4} \text{ m}^3/\text{s}$  with  
277 various numbers of baffles.

278

279 Each image is collected when the contents of the mixing were at steady state and is an average of  
280 several images together. The data collection time for a single image is around 30 ms. The  
281 tomographic image comprises  $20 \times 10$  pixels, which gives electrical conductivity dissemination  
282 information in both axial and radial directions. The accumulation of oxygen and its dispersal all over  
283 the sensing volume as the agitation rate increased was clearly identified. The blue colour shows  
284 background water, while the green colour represents low conductivity (less oxygen concentration) and  
285 red–yellow colour depicts high conductivity (more oxygen concentration) in the water.

286

287 Fig. 6(a) shows background measurement with the addition of one baffle, blue and green regions  
288 represent the distribution of very low electrical conductivity, reflecting the less dissolved oxygen  
289 within the sensing volume, it is also evident from Fig. 5 even after 1020 s the maximum oxygen  
290 concentration detected was 17.90 ppm. Fig. 6(b) images confirm that the addition of the second baffle  
291 to the vessel visibly identified; as the agitation is increased the deep blue colour is swapped by a red–  
292 yellow with time showing that the oxygen has well mixed within the sensing volume. As seen in Fig.  
293 6(b) and (c), there is not a significant difference between the pixels of the tomography images with  
294 two and three baffles, oxygen concentration increased only 0.30 ppm by changing two to three  
295 baffles. Fig. 6(d) represents the addition of the fourth baffle, which made a significant effect on  
296 mixing and the blue colour shade is completely replaced by red–yellow colour, even at the early  
297 stages, showing higher conductivity in terms of higher dissolved oxygen concentration in the vessel,  
298 reaching a maximum value of 19.98 ppm which is also shown in Fig. 5. This proves that there are less  
299 dead zones present in the case of four baffles as compared to one baffle. The results indicate that there  
300 is proper mixing by the use of a higher number of baffles.

301

302 For further more evidence, the conductivity data recorded during the experiments was also analysed  
303 and presented in Fig. 7, which indicate that conductivity values increase upon the oxygen absorption  
304 in the water.

305

306 Conductivity value increased from 0.297 S/m to 0.301 S/m with the addition of one baffle. Upon  
307 addition of the second and third baffle, the conductivity values of 0.302 S/m and 0.303 S/m were  
308 noticed respectively, which is a 0.3% addition to the value as compared to once baffle, which was  
309 1.3%. It is also evident from Fig. 5 that only the first baffle makes the significant difference in oxygen  
310 concentration in the mixing unit. A maximum conductivity value of 0.305 S/m was recorded with all  
311 four baffles, which is a 0.6% addition as compared to no baffling system.

## 312 **3.4 Optimisation and process economics**

### 313 **3.4.1 Gassed to un-gassed power measurements**

314 The gassed to un-gassed power ratio,  $P_g/P$  is plotted against the gas flow number,  $F_g$  for Rushton  
315 turbine impeller shown in Fig. 8. Increasing gas flow rate  $Q_g$  from 0 to  $8.5 \times 10^{-4}$  induce a fall in the  
316  $P_g/P$  ratio values from 1.0 to 0.4.

317

318 For small gas flow rate, a sudden decrease (about 20%) occurs at  $F_g$  value of 0.02, whereas for  
319 medium gas flow rate this decrease in the ratio of the  $P_g/P$  is comparatively slow. Lately at  $F_g$  value  
320 of 0.07 and above an average decrease of about 4.4% in the ratio of  $P_g/P$  was observed; which ends  
321 up with  $P_g/P$  value of 0.4 against  $F_g$ , 0.17. This fall in  $P_g/P$  with rising gas flow  $Q_g$  was linked with  
322 the evolving size of the gas occupied voids around the impeller blades, which has been  
323 comprehensively stated in the literature [26]. The power curve obtained is consistent with the one in  
324 the literature [27, 38]. The consistency of the power curve of the current study with literature shows  
325 that the methodology adopted to study gas-liquid mixing has valid applications in this area.

### 326 **3.4.2 Power consumption and system efficiency**

327 The cost of a gas-liquid mixing process mainly contingent on the power consumption. In order to  
328 make sure the best productivity, energy consumption must be optimised. The efficiency of the system  
329 could be defined as the function of gas concentrations and blend times [39]. Hence, the efficiency of  
330 the mixing unit is calculated from the time taken to achieve 17.90 ppm of oxygen concentration  
331 without and with different number of baffles. Fig. 9 depicts, even with only one baffle, time; 400 s  
332 spent was almost 1/3rd of the time when there was no baffle for mixing. The same amount of oxygen  
333 concentration was reached in 340 s with two and 320 s with three baffles, which is 67% and 73%  
334 improvement in the system efficiency, respectively. The system efficiency was 100%, while same  
335 concentration was reached in just 290 s for four baffles. With the addition of one, two, three and four  
336 baffles the system efficiency increased up to 50%, 67%, 73% and 100%, respectively, as compared to  
337 zero baffle system as the same level of performance is achieved in much shorter time.

338

339 The energy of the system is determined by using simple multiplication of operative power value with  
340 the time taken for complete mixing. As the number of baffles increased less energy is required to  
341 achieve maximum oxygen concentration. The energy requirement for complete mixing was 408 kJ in  
342 the case of no baffles. When the first baffle was introduced into the system, the consumption reduced  
343 to 272 kJ. Similarly, after the addition of the second and the third baffle the energy consumption was  
344 decreased to 244 kJ and 236 kJ which is about 70% increase in system efficiency. In the case of four  
345 baffles system's energy needed is measured as half. In short, as the extent of baffling in the system is  
346 increased, from un-baffled to one, two, three and four standard baffles, the energy requirement  
347 continually decreases and energy saving increases.

348

349 An economic analysis has also been applied to the current mixing unit and the results are presented in  
350 Fig. 10, which displays the influence of number of baffles on the cost of the baffles and the cost of  
351 energy input for the system. The cost of baffle here represents the cost of baffle plus its installation  
352 cost. With no baffle, the system requires high-energy input with which a high cost of energy  
353 production is associated as more power is required to mix the contents properly. In this case, there  
354 was no cost of the baffle. However, the energy input was the highest and same as its cost which was  
355 \$119. The introduction of one baffle introduced its cost into the system. The presence of this baffle  
356 helped to save a significant amount of the cost of energy input. The cost of the baffle was increased  
357 from \$0 to \$30, whereas the cost of energy input was decreased from \$119 to \$40. This introduced an  
358 increase of \$30 and a decrease of \$79 – a net saving of \$49 for each unit of energy input. The use of  
359 the second baffle further lowered the cost of energy input by \$20. However, the cost of the baffle has  
360 increased to \$62. Similarly, by increasing the number of baffles, the cost of baffles was increased.  
361 However, the cost of energy input was decreased significantly up to the fourth baffle as optimum  
362 mass transfer rates and mixing time was achieved at four numbers of baffles and less energy was  
363 required to obtain the same mass transfer rate.

364

365 In this economic analysis, the capital needed for the installation of baffles is the start-up capital and is  
366 the one-time expense only, whereas the cost of energy input is categorised as operating capital. With a  
367 maximum number of baffles, the cost of energy input is \$55 and the baffles cost is \$100. If the unit is  
368 made to operate for 20 hours a day, the operating cost would be \$1100 and the capital cost would be  
369 \$100. For no baffles, the cost of energy input is \$119 and the cost of baffles is \$0. This predicts an  
370 operating cost of \$2380 per day. Thus, the introduction of four baffles provides a total cost reduction  
371 of \$1280 per day. The results obtained are similar to the ones in the literature [40-42].

372

373 This part of paper studies the bare costs associated with liquid-gas mixing unit. However, the previous  
374 economic analysis in literature studies the full cost of mixing unit installation, scale-up of unit, cost of  
375 liquid in the vessel, the size of the plant, the cost associated with the mechanical failure of the unit  
376 (mechanical reliability failure) and maintenance cost, which we consider out of scope for the current  
377 study. Fig. 10 should also be analysed with the fact that the installation of baffles is a fixed-capital  
378 investment, once installed the system will provide a good mixing until its valuable life. Moreover, the  
379 cost of energy consumption is an operational cost. The study shows that a fixed-capital investment  
380 can save an amount of money, in terms of lowering the operational cost. The optimisation analysis  
381 shows that the minimum numbers of baffles required for the system are two, though this result  
382 depends on the dimensions of mixing tank under study.

## 383 **4. Conclusions**

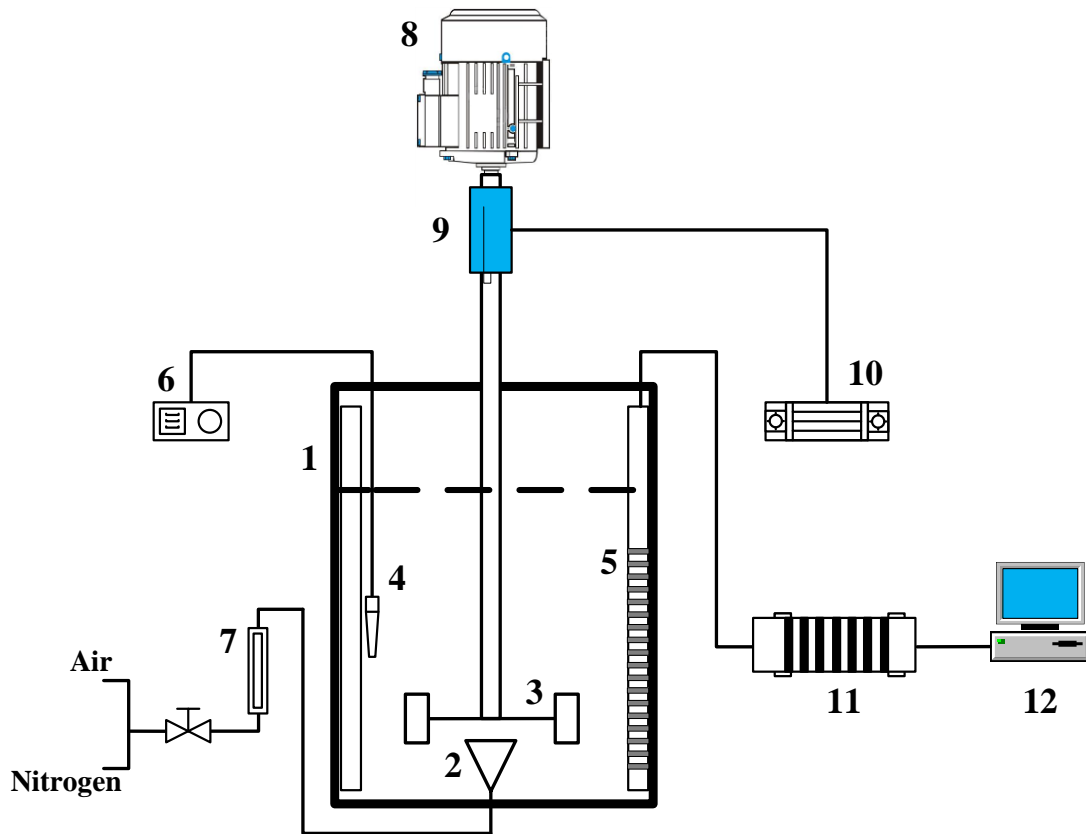
384 In this study, a major area of gas-liquid mixing was studied. It can be concluded that the tomography  
385 has the potential to be used as a modelling tool and diagnostic tool. This is also a general method of  
386 finding out what is occurring in process vessels. The ERT probe has been designed, manufactured and  
387 successfully tested, which can be used for the gas-liquid mixing analysis in stirred vessels and tanks  
388 routinely. The visualisation of the gas-liquid mixing in dynamic mixing has shown the behaviour of  
389 two different phases in the mixing vessel. The complete mixing process by adding the gas, its  
390 dispersion until it reaches the equilibrium concentration has been undertaken using the ERT. The

391 qualitative information on the flow and dispersion rates has been obtained by using different numbers  
392 of baffles through images at different times in the mixing vessel. The effects of vortex and number of  
393 baffles on the gas–liquid mixing rates have been analysed. The best mixing in shorter time was found  
394 while using four baffle systems. The energy consumed for full mixing was reduced to 204 kJ with  
395 100% system efficiency in terms of four baffles. The study also concluded that the operational cost  
396 would be at a minimum if the fixed capital investment is higher for the system. It is concluded from  
397 the observations that the use of four baffles optimises the process of mixing and the mixing can be  
398 completed with the shortest time and less operational cost. An economic analysis revealed that the use  
399 of an optimum number of baffles saved a cost of \$1280 per day. More than four baffles could give  
400 better results, hence it is recommended as a future work to use more than four baffles to find out the  
401 system performance. It is recommended to perform the mixing analysis using different temperature  
402 conditions inside the mixing unit and a model may be developed to see this effect on process  
403 economics. It is also suggested to perform such economic analysis with detailed cost analysis, keeping  
404 the factors, mentioned in economic analysis part, under considerations.

405

## 406 **Nomenclature**

407	$K_{La}$	mass transfer coefficient
408	$N_P$	power number
409	$Fr$	froude number
410	$F_g$	gas flow number
411	$N_{Re}$	reynolds number
412	$\rho$	fluid density ( $\text{kg m}^{-3}$ )
413	$\mu$	fluid viscosity ( $\text{kgm}^{-2}\text{s}^{-1}$ )
414	$Q_g$	gas flow rate ( $\text{m}^3 \text{s}^{-1}$ )
415	$g$	acceleration of gravity ( $\text{m s}^{-2}$ )
416	$T$	tank diameter (m)
417	$H$	liquid height (m)
418	$D$	impeller diameter (m)
419	$W$	blade width (m)
420	$N$	impeller speed ( $\text{s}^{-1}$ )
421		
422		

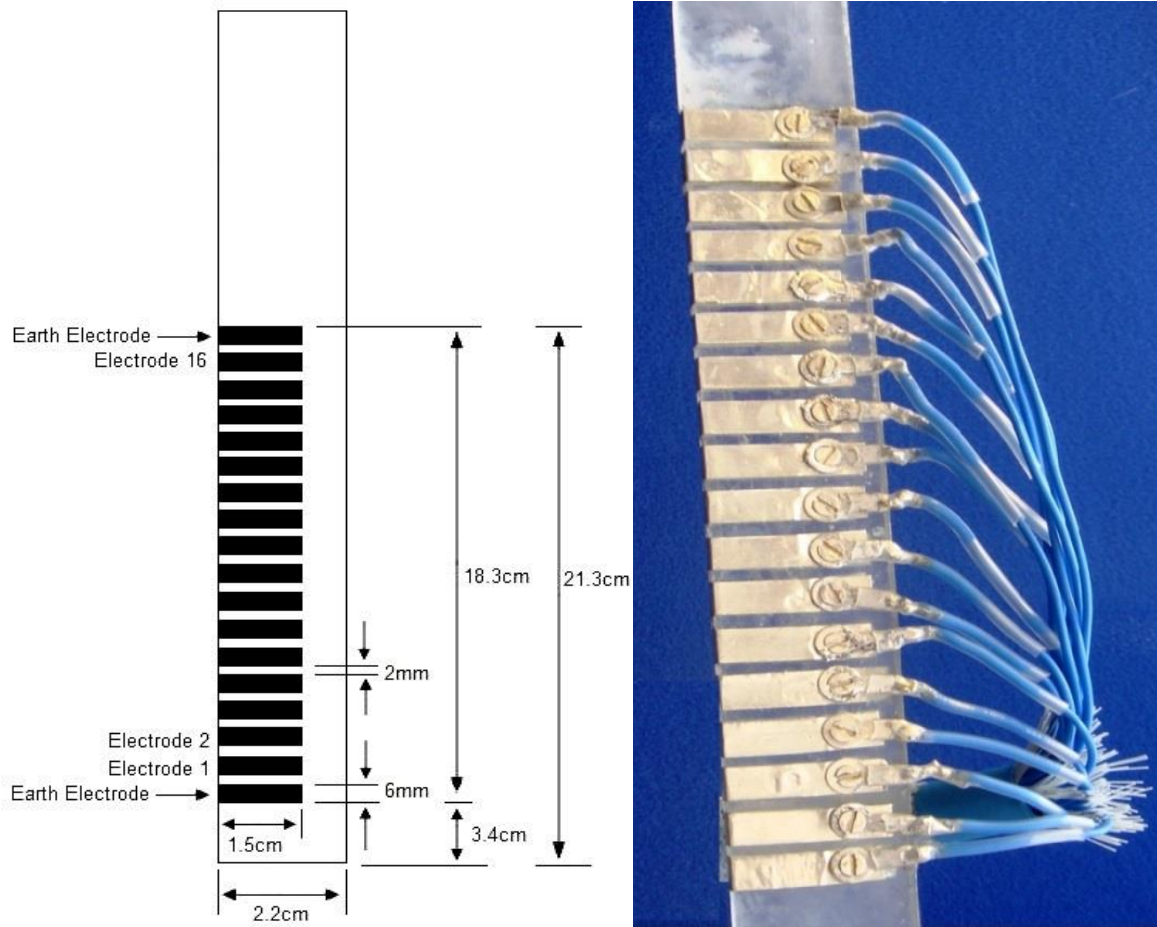


423

424 **Fig. 1.** Experimental setup: 1) Stirred vessel, 2) Gas sparger, 3) Impeller, 4) Oxygen probe, 5) ERT  
 425 probe and baffle, 6) Oxygen meter, 7) Rotameter, 8) Electric motor, 9) Torque meter assembly, 10)  
 426 Transducer, 11) Data acquisition system ITS, 12) Computer.

427

428



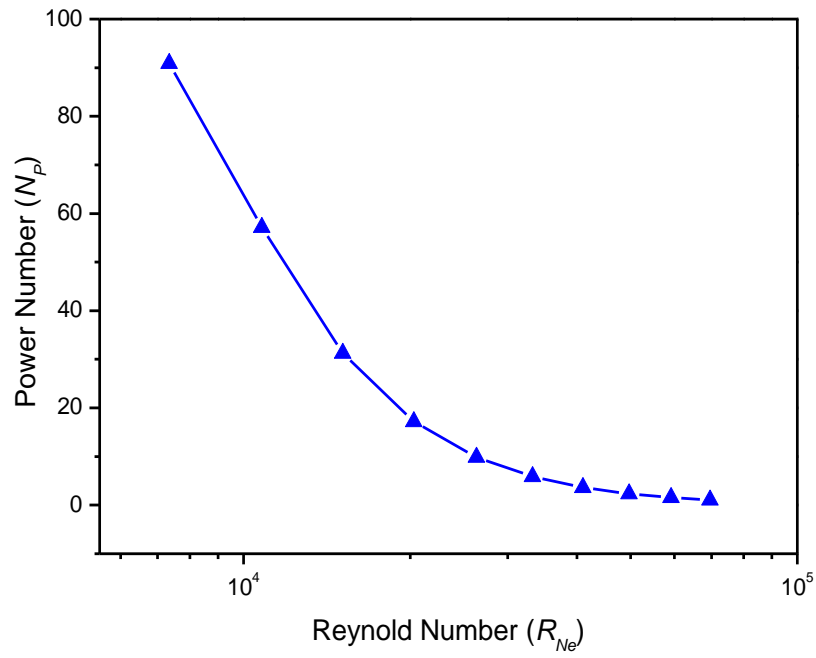
429

430

**Fig. 2.** Designed and constructed linear ERT probe.

431

432

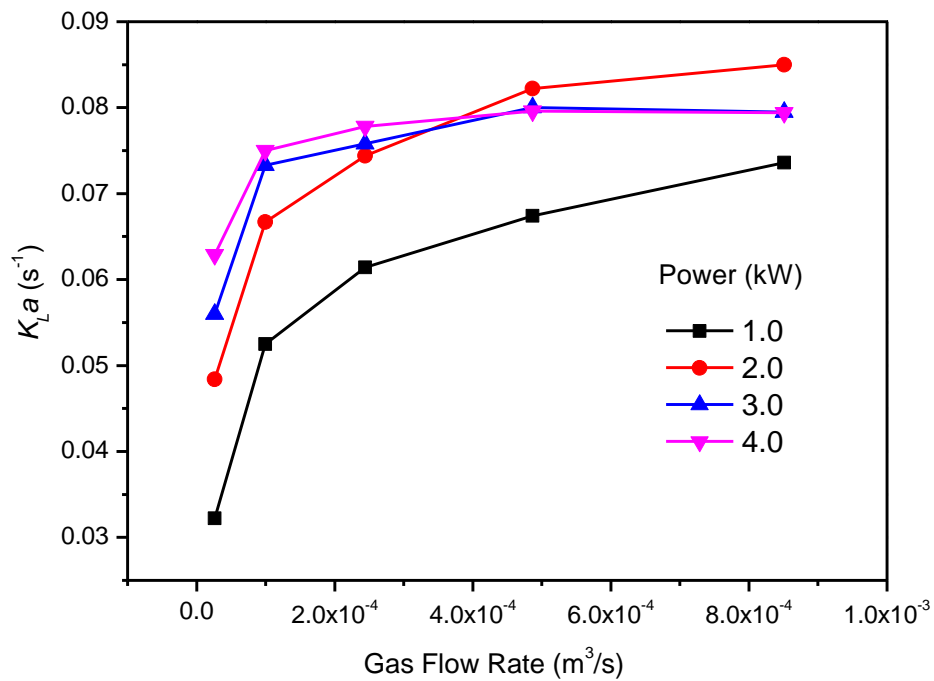


433

434 **Fig. 3.** Power number versus Reynolds number in the gas-liquid system using a Rushton turbine  
435 impeller.

436

437  
438



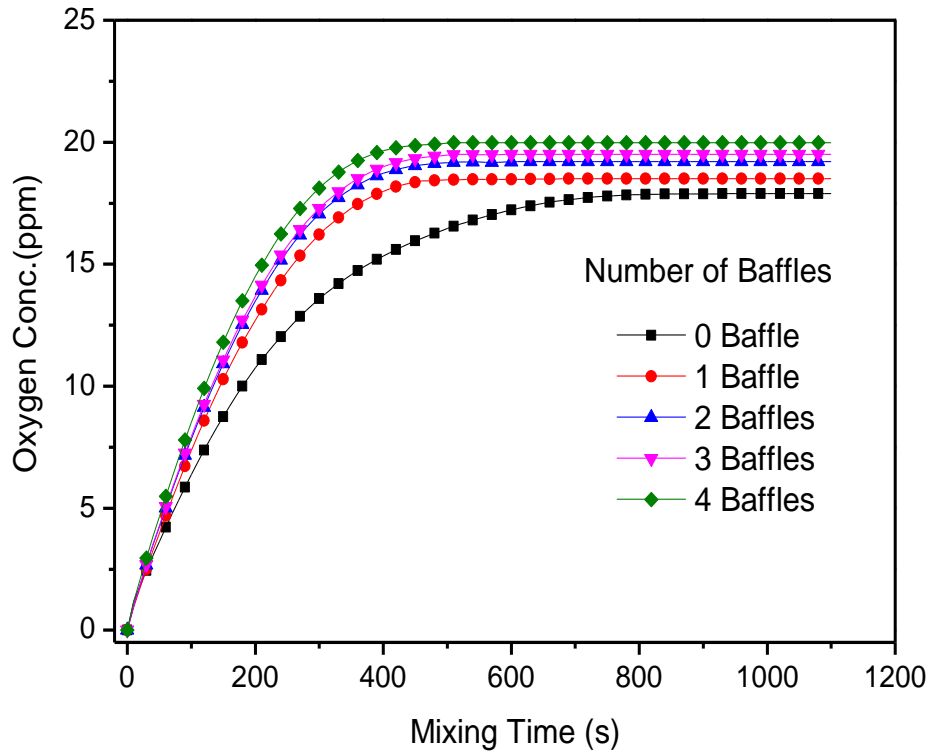
439

440

**Fig. 4.**  $K_L a$  values at various power and gas flow rates.

441

442



443

444

**Fig. 5.** Oxygen concentration against time with and without baffles in the mixing system.

445

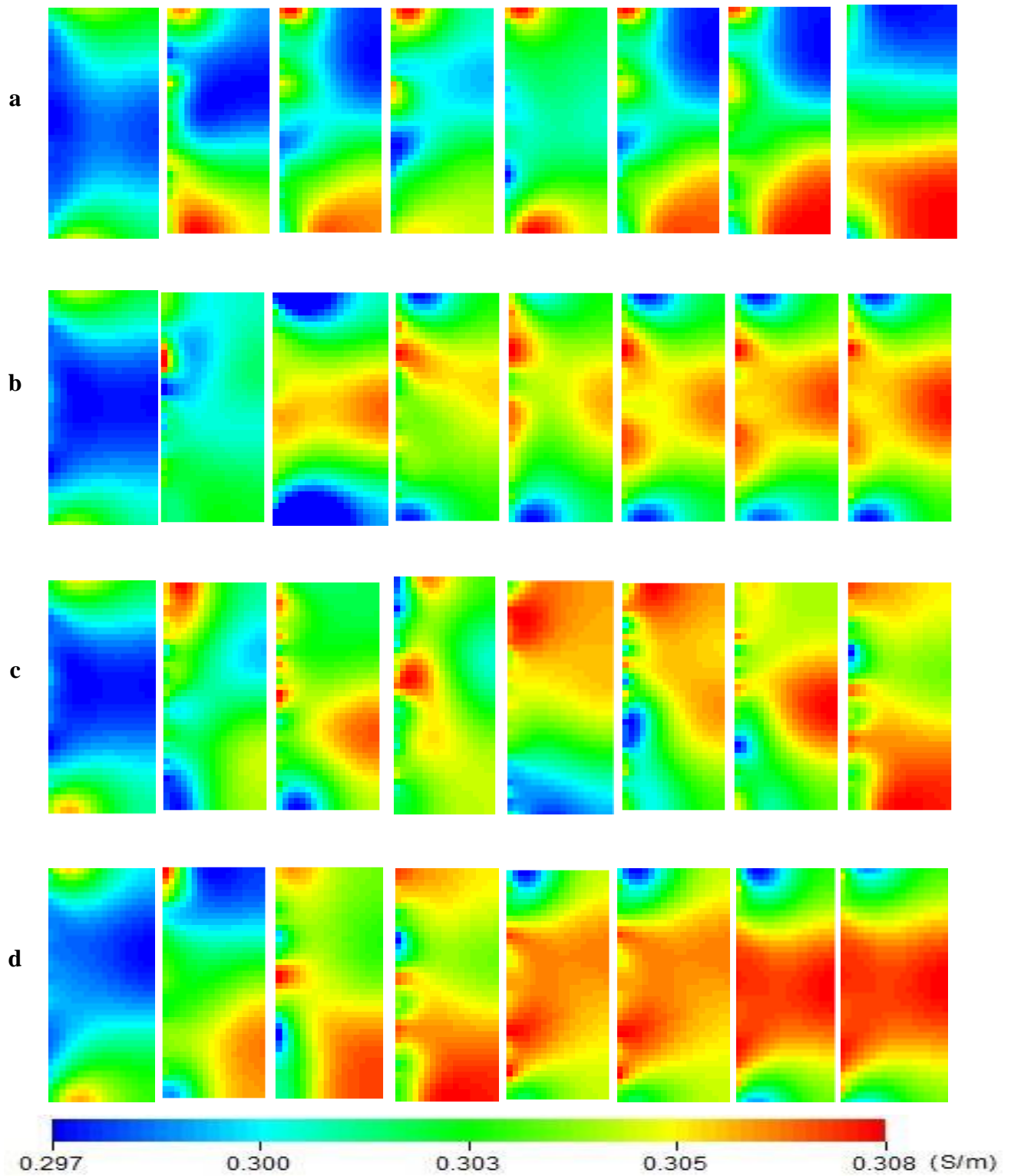
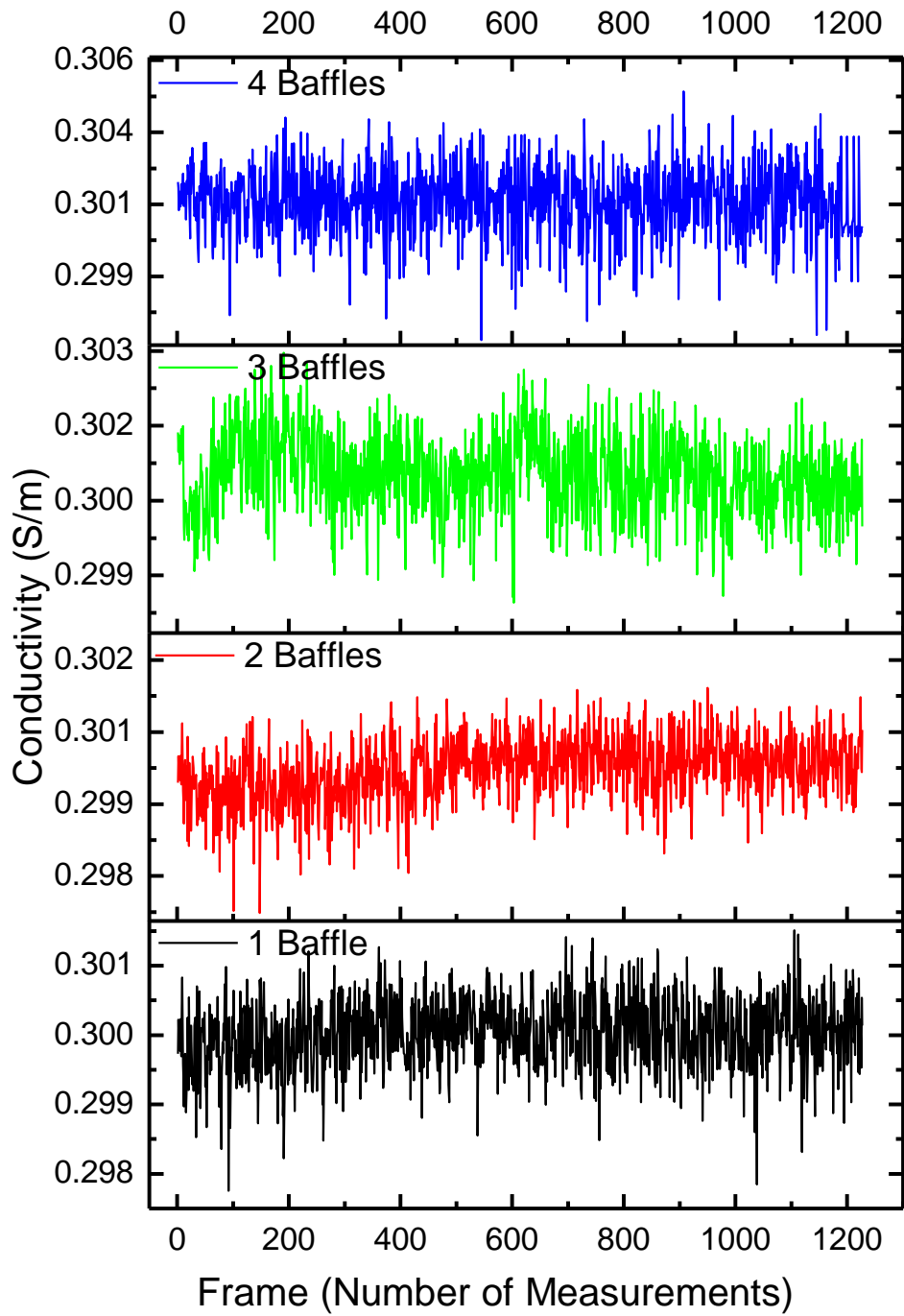


**Fig. 6.** Comparison of tomographic images with a) one, b) two, c) three and d) four baffles during gas-liquid mixing at the optimum power of 2.0 kW and gas flow rate  $8.5 \times 10^{-4} \text{ m}^3/\text{s}$ .

451  
452

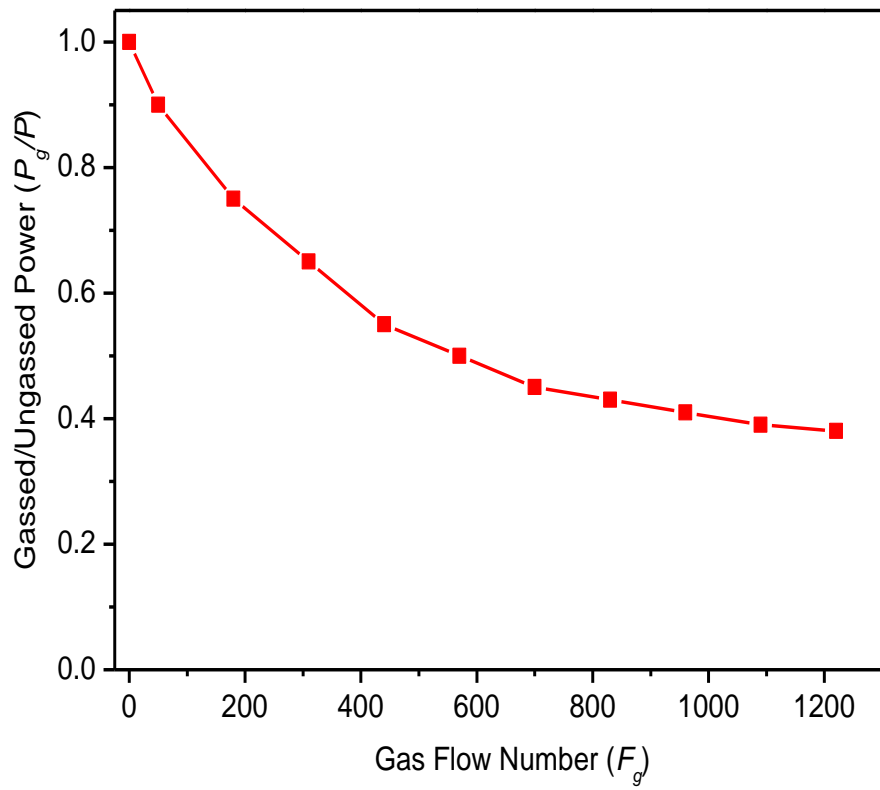


453

454 **Fig. 7.** Conductivity planes against the number of measurements with one, two, three and four  
455 baffles.

456

457



458

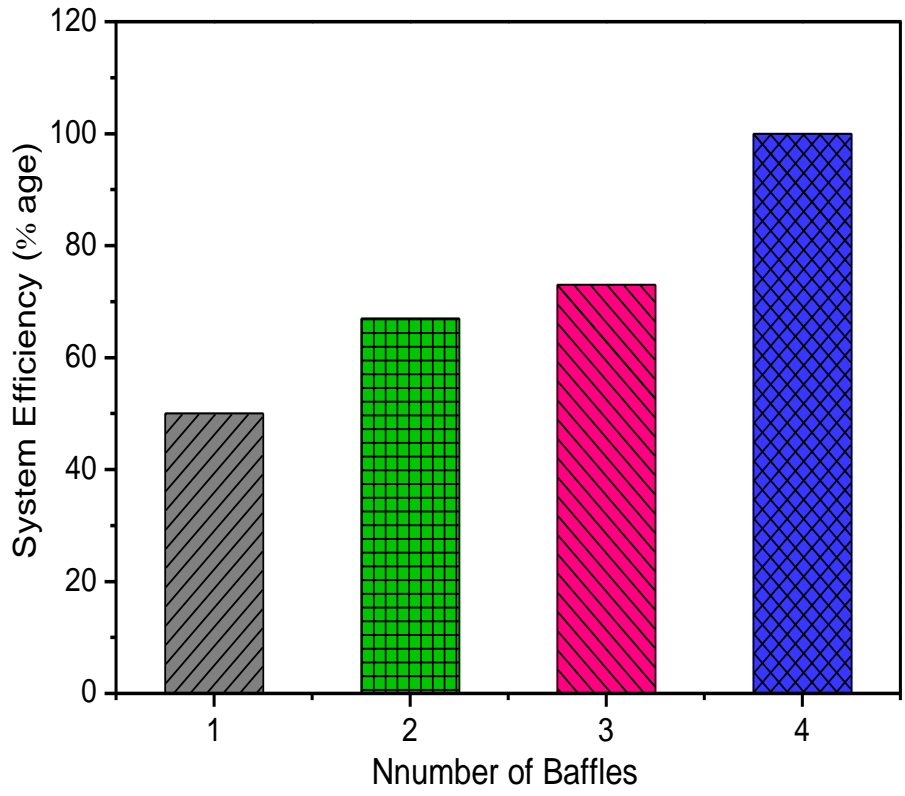
459

**Fig. 8.** Evaluation of the gassed to un-gassed power ratio with rising gas flow rate.

460

461

462



463

464 **Fig. 9.** Improving mixing unit efficiency by increasing the number of baffles.

465

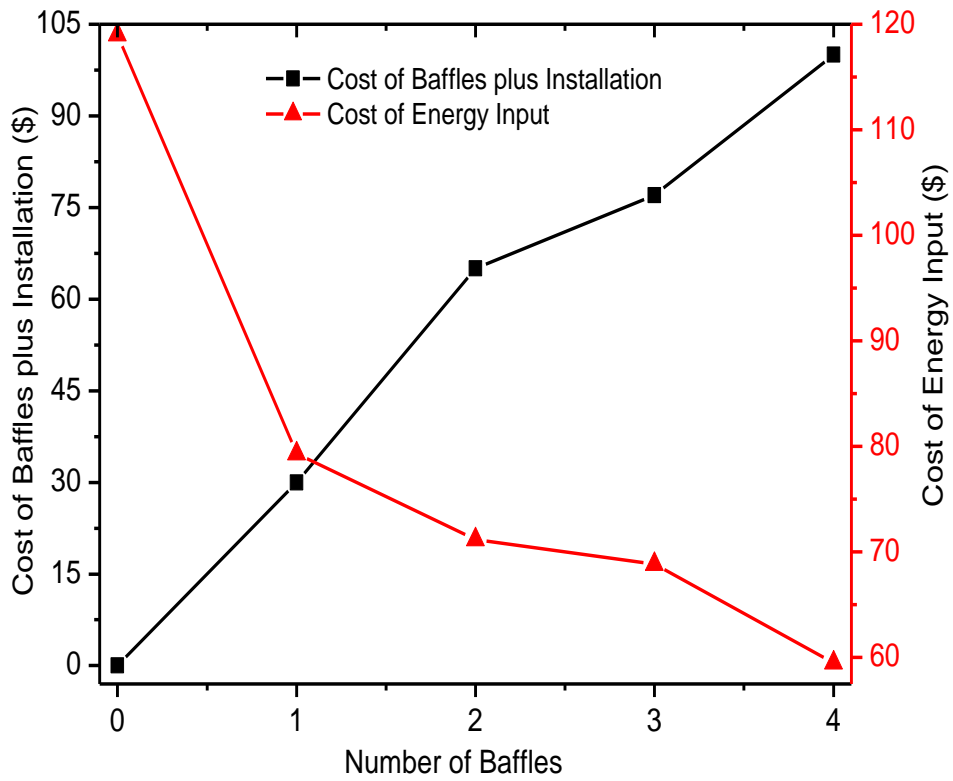


**Fig. 10.** Cost analysis of the gas-liquid mixing unit.

## References

1. Kleerebezem, R. and M.C. van Loosdrecht, Mixed culture biotechnology for bioenergy production. *Current opinion in biotechnology*, 2007. 18(3): p. 207-212.
2. Paul, E.L., V.A. Atiemo-Obeng, and S.M. Kresta, *Handbook of industrial mixing: science and practice*. 2004: John Wiley & Sons.
3. Moinfar, S. and M.-R.M. Hosseini, Development of dispersive liquid–liquid microextraction method for the analysis of organophosphorus pesticides in tea. *Journal of hazardous materials*, 2009. 169(1): p. 907-911.
4. Assirelli, M., et al., Macro-and micromixing studies in an unbaffled vessel agitated by a Rushton turbine. *Chemical Engineering Science*, 2008. 63(1): p. 35-46.
5. Lane, G., M. Schwarz, and G. Evans, Numerical modelling of gas–liquid flow in stirred tanks. *Chemical Engineering Science*, 2005. 60(8): p. 2203-2214.
6. Micheletti, M., et al., Fluid mixing in shaken bioreactors: Implications for scale-up predictions from microlitre-scale microbial and mammalian cell cultures. *Chemical Engineering Science*, 2006. 61(9): p. 2939-2949.
7. Kapic, A. and T. Heindel, Correlating gas-liquid mass transfer in a stirred-tank reactor. *Chemical Engineering Research and Design*, 2006. 84(3): p. 239-245.
8. Tribe, L., C. Briens, and A. Margaritis, Determination of the volumetric mass transfer coefficient (kLa) using the dynamic “gas out–gas in” method: Analysis of errors caused by dissolved oxygen probes. *Biotechnology and bioengineering*, 1995. 46(4): p. 388-392.
9. Moutafchieva, D., et al., Experimental determination of the volumetric mass transfer coefficient. *Journal of Chemical Technology & Metallurgy*, 2013. 48(4).
10. Wang, F. and Z.-S. Mao, Numerical and experimental investigation of liquid-liquid two-phase flow in stirred tanks. *Industrial & engineering chemistry research*, 2005. 44(15): p. 5776-5787.
11. Lane, G., M. Schwarz, and G. Evans, Predicting gas–liquid flow in a mechanically stirred tank. *Applied Mathematical Modelling*, 2002. 26(2): p. 223-235.
12. Yapici, K., et al., Numerical investigation of the effect of the Rushton type turbine design factors on agitated tank flow characteristics. *Chemical Engineering and Processing: Process Intensification*, 2008. 47(8): p. 1340-1349.
13. Lamberto, D., et al., Using time-dependent RPM to enhance mixing in stirred vessels. *Chemical Engineering Science*, 1996. 51(5): p. 733-741.
14. Kresta, S.M. and P.E. Wood, The flow field produced by a pitched blade turbine: characterization of the turbulence and estimation of the dissipation rate. *Chemical Engineering Science*, 1993. 48(10): p. 1761-1774.

15. Adrian, R.J., Twenty years of particle image velocimetry. *Experiments in Fluids*, 2005. 39(2): p. 159-169.
16. Roehle, I., et al., Recent developments and applications of quantitative laser light sheet measuring techniques in turbomachinery components. *Measurement Science and Technology*, 2000. 11(7): p. 1023.
17. Schäfer, M., M. Höfken, and F. Durst, Detailed LDV measurements for visualization of the flow field within a stirred-tank reactor equipped with a Rushton turbine. *Chemical Engineering Research and Design*, 1997. 75(8): p. 729-736.
18. Pettersson, M. and Å.C. Rasmuson, Hydrodynamics of suspensions agitated by pitched-blade turbine. *AIChE journal*, 1998. 44(3): p. 513-527.
19. Carletti, C., et al., Analysis of solid concentration distribution in dense solid–liquid stirred tanks by electrical resistance tomography. *Chemical Engineering Science*, 2014. 119: p. 53-64.
20. Aw, S.R., et al., Electrical resistance tomography: A review of the application of conducting vessel walls. *Powder Technology*, 2014. 254: p. 256-264.
21. Yenjaichon, W., et al., Mixing quality in low consistency fibre suspensions downstream of an in-line mechanical mixer measured by electrical resistance tomography. *Nordic Pulp and Paper Research Journal*, 2014. 29(3): p. 392-400.
22. Abdullah, B., et al., Electrical resistance tomography-assisted analysis of dispersed phase hold-up in a gas-inducing mechanically stirred vessel. *Chemical Engineering Science*, 2011. 66(22): p. 5648-5662.
23. Yenjaichon, W., et al., Assessment of mixing quality for an industrial pulp mixer using electrical resistance tomography. *The Canadian Journal of Chemical Engineering*, 2011. 89(5): p. 996-1004.
24. Tahvildarian, P., et al., Using electrical resistance tomography images to characterize the mixing of micron-sized polymeric particles in a slurry reactor. *Chemical Engineering Journal*, 2011. 172(1): p. 517-525.
25. Hosseini, S., et al., Study of solid–liquid mixing in agitated tanks through electrical resistance tomography. *Chemical Engineering Science*, 2010. 65(4): p. 1374-1384.
26. Hari-Prajitno, D., et al., Gas-liquid mixing studies with multiple up-and down-pumping hydrofoil impellers: Power characteristics and mixing time. *The Canadian Journal of Chemical Engineering*, 1998. 76(6): p. 1056-1068.
27. Coulson, J.M., et al., *Coulson and Richardson's Chemical Engineering Volume 1 - Fluid Flow, Heat Transfer and Mass Transfer (6th Edition)*. 1999, Elsevier.
28. Dickin, F. and M. Wang, Electrical resistance tomography for process applications. *Measurement Science and Technology*, 1996. 7(3): p. 247.

29. Mann, R., et al. Resistance tomography imaging of stirred vessel mixing at plant scale. in Institution of chemical engineers symposium series. 1996. Hemisphere publishing corporation.
30. Beck, M.S., Process tomography: principles, techniques and applications. 1995: Butterworth-Heinemann.
31. Gladden, L., Process Tomography: Principles, Techniques and Applications. Measurement Science and Technology, 1997. 8(4).
32. Mann, R., et al., Application of electrical resistance tomography to interrogate mixing processes at plant scale. Chemical Engineering Science, 1997. 52(13): p. 2087-2097.
33. Peters, M.S. and K.D. Timmerhaus, Plant design and economics for chemical engineers. 2002, New York: McGraw-Hill.
34. Towler, G.P. and R.K. Sinnott, Chemical engineering design: principles, practice, and economics of plant and process design. 2013: Elsevier.
35. Hockey, R. and J. Nouri, Turbulent flow in a baffled vessel stirred by a 60 pitched blade impeller. Chemical Engineering Science, 1996. 51(19): p. 4405-4421.
36. Myers, K.J., M.F. Reeder, and J.B. Fasano, Optimize mixing by using the proper baffles. Chem. Eng. Prog, 2002. 98(2): p. 42-47.
37. Wang, M., et al., Measurements of gas-liquid mixing in a stirred vessel using electrical resistance tomography (ERT). Chemical Engineering Journal, 2000. 77(1): p. 93-98.
38. Sardeing, R., et al., Gas-Liquid Mass Transfer: Influence of Sparger Location. Chemical Engineering Research and Design, 2004. 82(9): p. 1161-1168.
39. Nienow, A.W., M.F. EDWARDS, and N. Harnby, Mixing in the process industries. 1997: Butterworth-Heinemann.
40. Nienow, A.W., M.F. Edwards, and N. Harnby, eds. Mixing in the Process Industries. second ed. 1997, Butterworth Heinemann.
41. Kenney, W.F., Energy Conservation in the Process Industries. Elsevier Science.
42. Gubanov, O. and L. Cortelezzi, On the cost efficiency of mixing optimization. Journal of Fluid Mechanics. 692: p. 112-136.